frontiers | Frontiers in Energy Research

ORIGINAL RESEARCH
published: 01 April 2022
doi: 10.3389/fenrg.2022.879373

Optimal Sizing Grid-Connected Hybrid PV/Generator/Battery Systems Following the Prediction of CO_2 Emission and Electricity Consumption by Machine Learning Methods (MLP and SVR): Aseer, Tabuk, and Eastern Region, Saudi Arabia

Khalid Almutairi[1], *Mubarak Almutairi*[2], *Kamal Harb*[3]* *and Omar Marey*[2]

[1]Applied College, Mechanical Engineering Technology, University of Hafr Al Batin, Hafr Al Batin, Saudi Arabia, [2]College of Computer Science & Engineering, University of Hafr Al Batin, Hafr Al Batin, Saudi Arabia, [3]Electrical Engineering, University of Hafr Al Batin, Hafr Al Batin, Saudi Arabia

OPEN ACCESS

Edited by:
Sorour Alotaibi,
Kuwait University, Kuwait

Reviewed by:
Morteza Fahimalavi,
Sharif University of Technology, Iran
Misagh Irandoostshahrestani,
University of Tehran, Iran

***Correspondence:**
Kamal Harb
kharb@uhb.edu.sa

Specialty section:
This article was submitted to Process and Energy Systems Engineering, a section of the journal Frontiers in Energy Research

Received: 19 February 2022
Accepted: 09 March 2022
Published: 01 April 2022

Citation:
Almutairi K, Almutairi M, Harb K and Marey O (2022) Optimal Sizing Grid-Connected Hybrid PV/Generator/Battery Systems Following the Prediction of CO_2 Emission and Electricity Consumption by Machine Learning Methods (MLP and SVR): Aseer, Tabuk, and Eastern Region, Saudi Arabia. Front. Energy Res. 10:879373. doi: 10.3389/fenrg.2022.879373

Researchers' concentration has been on hybrid systems that can fulfill economic and environmental goals in recent years. In this study, first, the prediction of CO_2 emission and electricity consumption of Saudi Arabia by 2040 is made by employing multi-layer perceptron (MLP) and support vector regression (SVR) methods to see the rate of CO_2 emission and electricity consumption. In this regard, the most important parameters such as gross domestic product (GDP), population, oil consumption, natural gas consumption, and renewable consumption are considered. Estimating CO_2 emission by MLP and electricity consumption by SVR showed 815 Mt/year and 475 TWh/year, respectively, where R2 for MLP and SVR was 0.99. Prediction results showed a 31% and 39% increase in CO_2 emission and electricity consumption by 2040 compared to 2020. Second, the optimum combination of components for supplying demand load and desalination load in residential usages are found where 0% capacity shortage, 20–60$/t penalty for CO_2 emission, sell back to the grid, and both fixed and random grid outages are considered. Load demands were considered under two winter and non-winter times so that 4,266, 2,346, and 3,300 kWh/day for Aseer, Tabuk, and the Eastern Region were shown, respectively. Results show that 0.12, 0.11, and 0.12 (kW (PV))/(kWh/day(load)) and 0.1, 0.08, and 0.08 (kW(Bat))/(kWh/day(load)) are required under the assumption of this study for Aseer, Tabuk, and the Eastern Region, respectively. Also, COEs for the proposed systems are 0.0934, 0.0915, and 0.0910 $/kWh for Aseer, Tabuk, and the Eastern Region, respectively. Also, it was found that renewable fractions (RFs) between 46% and 48% for all of the case studies could have rational COE and NPCs and fulfill the increasing rate of CO_2 emission and electricity consumption. Finally, sensitivity analysis on grid CO_2 emission and its penalty, load and solar Global Horizontal Irradiance (GHI), PV, and battery prices

showed 45%–55%, 42%–52%, and 43%–49% RFs for Aseer, Tabuk, and the Eastern Region, respectively.

Keywords: machine learning, MLP, SVR, HOMER, renewable, CO_2 prediction, electricity prediction

1 INTRODUCTION

Increasing the world's population and energy consumption would lead researchers to find techno-economical solutions for reducing greenhouse gases, especially CO_2, following the use of fossil fuels. For sure, renewables such as solar, wind, hydro, geothermal (Sayed et al., 2021), fuel cells, etc., are among the best available solutions with enough resources (Forootan Fard et al., 2020). Furthermore, hybrid systems using various resources would lead to more reliable energy systems and more flexible power supply systems than single-source systems (Tee et al., 2016). The share of renewables in the world's power generation was 28.6% in 2020, while this value for 2010 was 19.91%. Despite the increasing share of renewables, total CO_2 emission increased from 30.4 Gt in 2010 to 31.5 Gt in 2020 (IEA, 2021). It means that the share of clean energies in power generation should be increased as well as other feasible energy saving methods.

It is no secret that electricity consumption depends on such major factors as population, air temperature, gross domestic product (GDP), etc. Also, CO_2 emission depends on fossil fuel consumption, which is directly connected with GDP, electricity consumption, and other factors (Nishan, 2020; Altikat, 2021; Bamisile et al., 2021; Qu et al., 2021; Xu et al., 2021). One of the issues regarding the design of power supply systems is having an estimation of needed electricity, and if the reduction of CO_2 is essential, having its accurate and appropriate estimation (Ibrahim et al., 2020; Ming et al., 2020). In this regard, artificial intelligence methods such as machine learning methods could be a rational option (Shabani et al., 2021).

Ghalandari et al. (2020) predicted CO_2 emission of four European countries by employing MLP and group method of data handling (GMDH) and concluded that both methods were well aligned for forecasting based on their R2 (0.99) and preferred MLP to GMDH due to its lower error value. Mamdouh El Haj Assad et al. (2021) used the MLP method for the prediction of CO_2 emission of Middle Eastern countries and concluded that the logsig transfer function for the hidden layer has a high R2 (0.99) and low mean absolute error (MSE). Heydari et al. (2019) used different ANN methods such as MLP and RBF to forecast the CO_2 emission of Iran, Italy, and Canada. Their results showed that MLP and other employed methods have acceptable accuracy according to the obtained mean absolute error. Zhu et al. (2020) predicted peak values of CO_2 emission of China for the transportation industry by using SVR and obtained very low MSE, showing the accuracy of their model. Singh et al. (2021) considered random forest regressor, SARIMAX, Holt-Winters (H-W), and SVR to predict CO_2 emission from the paddy crop in India and found that H-W and SVR had a lower value of MSE than other methods.

1.1 An Overview of Saudi Arabia's Energy System

Saudi Arabia is in the Middle East, where the weather is warm and dry. It holds 15% of the world's oil reserves. Ten quadrillion British thermal units of total primary energy in 2020 were consumed in this country, where oil and natural gas were 62% and 38% of the country's total energy consumption, respectively. In the central and eastern parts of this country, most of the electricity generation is from natural gas, while due to the lack of accessibility to natural gas in the western part, power production is dependent on petroleum liquids (U.S. EIA, 2021). Although the share of renewable energies for power generation is meager, this country has provided some significant plans for installing solar systems to diversify power supply systems and reduce greenhouse gas emissions. Hence, studying the current energy system and investigating some of the most important related trends in population, GDP, electricity, and CO_2 emission and providing technical and economical solutions for using hybrid renewable systems seem essential (Barhoumi et al., 2020; Taylan et al., 2020).

Renewable energies are essential for Gulf Cooperation Council (GCC) countries such as Saudi Arabia, and different renewable resources can provide a significant part of needed energy in the form of hybrid off/on-grid systems (Almasri and Narayan, 2021). Bilal Awan (2019) investigated an off/grid hybrid system with various sizes of components and concluded that a combination of DG/WT/PV/Bat systems has the best performance, as it has a COE of 0.164 ($/kWh) and led to reduction of CO_2 by 46.5% compared to the only diesel system. Tazay (2020) studied grid-connected hybrid systems including PV/Wind/Bat for energy supply in different cities of Saudi Arabia, including Tabuk, and considering the current electricity tariffs, concluded that the grid/PV system is the best choice with the COE of 0.0688 ($/kWh), where RF is 50% and will reduce CO_2 emission by 54.3%. Alharthi et al. (2018) optimized grid-connected PV/Wind systems and found it economical compared to the only grid without any renewable system, considering the CO_2 emission of both systems. Other hybrid renewable systems are presented in **Table 1**.

Considering the growth rate of CO_2 emission and electricity consumption in designing hybrid systems is an important issue not seen in similar studies. Also, considering the combination of planned and random outages in peak hours to find the optimum ranges of RFs for the case study regions could lead to filling previous gaps in the studies mentioned in the literature review. In this research, as the first step, machine learning methods such as multi-layer perceptron (MLP) and support vector regression (SVR) are employed to predict CO_2 emission and electricity

TABLE 1 | Renewable hybrid systems in Saudi Arabia.

References	City	Power usage	Hybrid system	Grid	COE ($/kWh)	RF (%)
Tazay et al. (2020)	Al Baha	University	PV/WT//Bat/FC	Off-grid	0.289	100
Salameh et al. (2021)	Neom	Industry	PV/DG/Bat	On-grid	0.4	95
Awan et al. (2019)	Sharurah	Residential	PV/DG/Bat	On-grid	0.178	37
Kharrich et al. (2021)	Yanbu	Residential	PV/Biomass	Off-grid	0.208	100
Seedahmed et al. (2022)	Makkah	Residential	WT/DG/FC/Bat	Off-grid	0.271	100
Dehwah and Krarti, (2019)	Eastern Region	Residential	PV/WT	On-grid	0.143	32
Al Garni et al. (2018)	Makkah	Residential	PV	On-grid	0.049	35

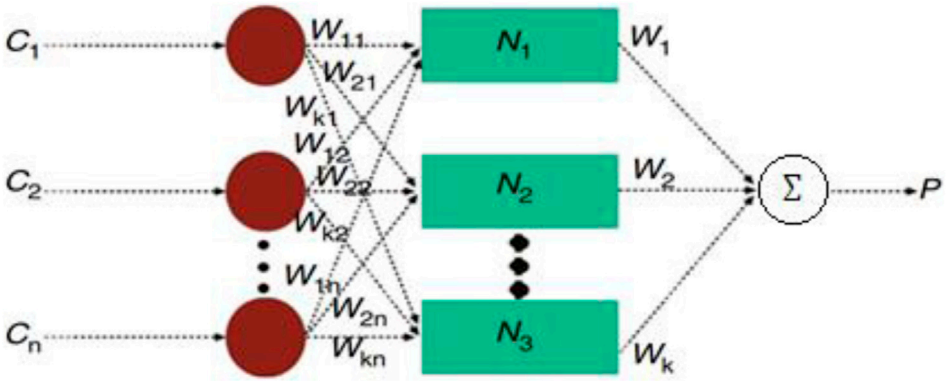

FIGURE 1 | Schematic of the MLP method.

consumption for Saudi Arabia by 2040. The obtained results show the importance of using renewable energies according to the variation of CO_2 emission and electricity consumption rates. Then, considering some assumed grid blackouts in the peak hours of days to supply the demand load by renewables and reduce pressure on the grid at these times, optimum renewable hybrid systems are designed for Aseer, Tabuk, and the Eastern Region of Saudi Arabia as the three different coastal regions in this country. As the final step, sensitivity analysis on the social cost of CO_2 emission coupled with different amounts of emissions, sensitivity analysis on the load connected with solar global horizontal irradiance (GHI), and sensitivity analysis on the amount of PV and battery prices are considered to see the optimum RF and NPC changes for two main purposes: first, generalizing the results for all of the coastal regions of the country, and second, generalizing the results for other parts of the world, especially for the neighbor countries, with similar or different weather conditions.

2 MACHINE LEARNING (MLP AND SVR)

The following presents the structure of the MLP and SVR methods and their characteristics. For both of them, mean absolute error (MAE) is calculated through **Eq. 1**, where n is the number of samples, Y is the real output, and Ŷ is the predicted output (Zhang et al., 2021).

$$MAE = \frac{1}{n}\sum_{i=1}^{n}\left|Y - \hat{Y}\right| \tag{1}$$

2.1 MLP

MLP is considered as a supervised learning method including some neurons and hidden layers which are determined according to the complexity of the model based on inputs (X), the number of features (X: [f_1, f_2, …, features]), and their correlation and outputs (Y: [y_1, y_2, …]. **Figure 1** shows the structure of this neural network (Ramezanizadeh et al., 2019). Neurons in the hidden layers apply coefficients on the inputs and a function to transform the values into the outputs. Also, MLP uses the square error loss function as in **Eq. 2**, where W is the weight matrix, Ŷ is the predicted value, Y is the actual value, and α is its hyperparameter.

$$Loss(\hat{y}, y, W) = \frac{1}{2}\left\|\hat{y} - y\right\|_2^2 + \frac{\alpha}{2}\left\|W\right\|_2^2 \tag{2}$$

2.2 SVR

SVR is one of the support vector machine's (SVM) forms. This method's separation of input data is based on different lines or surfaces (kernels), as shown in **Figure 2A** (Singh et al., 2020), which are used for training the model for the following predictions. The structure of SVMs is demonstrated in **Figure 2B** (Buyukyildiz et al., 2013).

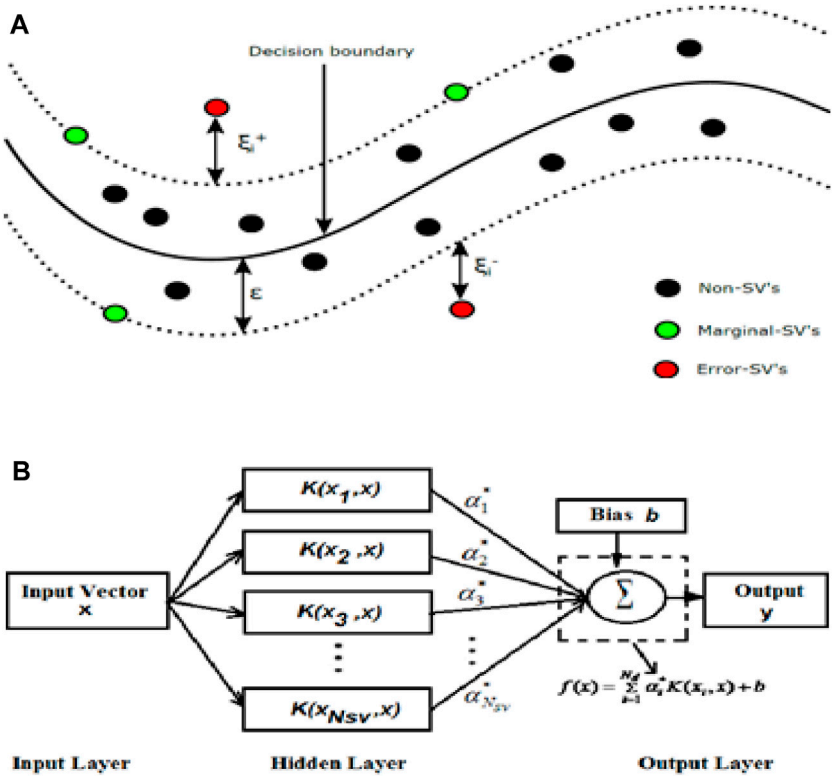

FIGURE 2 | (A) A kind of kernel employed in the SVR method. **(B)** General structure of support vector machines.

2.3 Prediction of CO_2 Emission by 2040

This part presents the most influential parameters on CO_2 emission and their trend by 2040, along with optimized input parameters of MLP and SVR models. For the prediction of CO_2 emission, the most important parameters such as GDP, oil consumption, natural gas consumption, and renewable consumption are considered as inputs' features. **Figures 3A–D** show the values of selected features from 1980 to 2019 along with their assumed values till 2040 based on employed appropriate trend lines and their R2 as an accuracy criterion.

2.4 Prediction of Electricity Consumption by 2040

For prediction of electricity consumption, goal consumption, population, air temperature, unemployment rate, and renewables are considered as inputs' features. **Figures 3E–H** show the mentioned feature values from 1980 to 2019 and their predicted values based on trend lines.

2.5 Hybrid System Modeling

In the following, an introduction of the case studies, load profiles, and proposed hybrid system are presented.

2.5.1 Characteristics of the Case Studies

Figure 4 shows Saudi Arabia and the case study regions. As can be seen, selected case studies, including Aseer, Tabuk, and the Eastern Region, are all in the coastal parts of the country.

2.5.2 Aseer

As it can be seen in **Figure 4**, Aseer is one of the southwest provinces of Saudi Arabia. According to a household energy survey conducted in 2017 (Survey, 2017), the number of households in this province is 398,969, and total electricity consumption was 10.9 billion kWh/year. Hence, each household used 75 kWh/day on average, that is, 29 kWh/day in winter and 47 kWh/day for the rest of the year. The latitude and longitude of the selected case study region are 19°N, 42°E, respectively.

Figure 5A presents a deferrable load of 140 kWh/day in total so that water usage is assumed to be 0.07 m^3/day for each person and 4 kWh/m^3 for desalination (Wu et al., 2018; Eltamaly et al., 2021), and the demanded load of 2,850 kWh/day in winter months (January-February-December) and 4,680 kWh/day for the rest of the year is scaled on the defined distribution of residential usage in HOMER software. As it can be seen, peak times occur from June to September, and it is evident that this happens between 1 and 6 p.m., known as peak times in Saudi Arabia. Also, **Figure 5B** shows solar radiation with an average of 5.97 kWh/m^2/day for this province, which is very good as a renewable resource.

2.5.3 Tabuk

Tabuk is located in the northwest of Saudi Arabia, as shown in **Figure 4**, where the number of its households was 166,845, and total electricity consumption was 2.6 billion kWh/year.

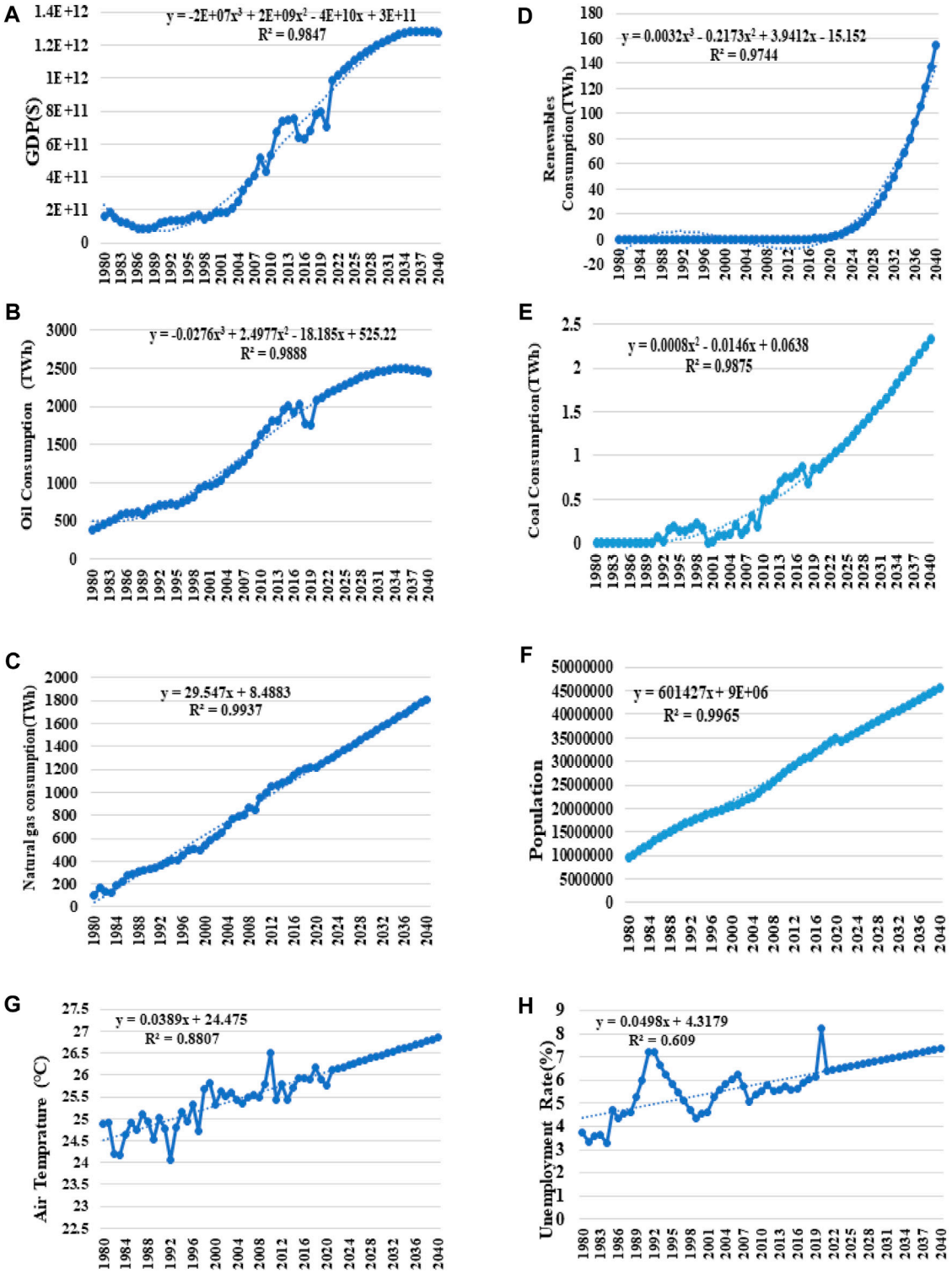

FIGURE 3 | (A) Estimation of GDP by 2040 based on trend line. **(B)** Estimation of oil consumption based on trend line. **(C)** Estimation of natural gas consumption by 2040 based on trend line. **(D)** Estimation of renewable consumption based on trend line. **(E)** Estimation of coal consumption by 2040 based on trend line. **(F)** Estimation of population by 2040 based on trend line. **(G)** Estimation of air temperature by 2040 based on trend line. **(H)** Estimation of the unemployment rate by 2040 based on trend line.

FIGURE 4 | Overview of Saudi Arabia and the case study regions.

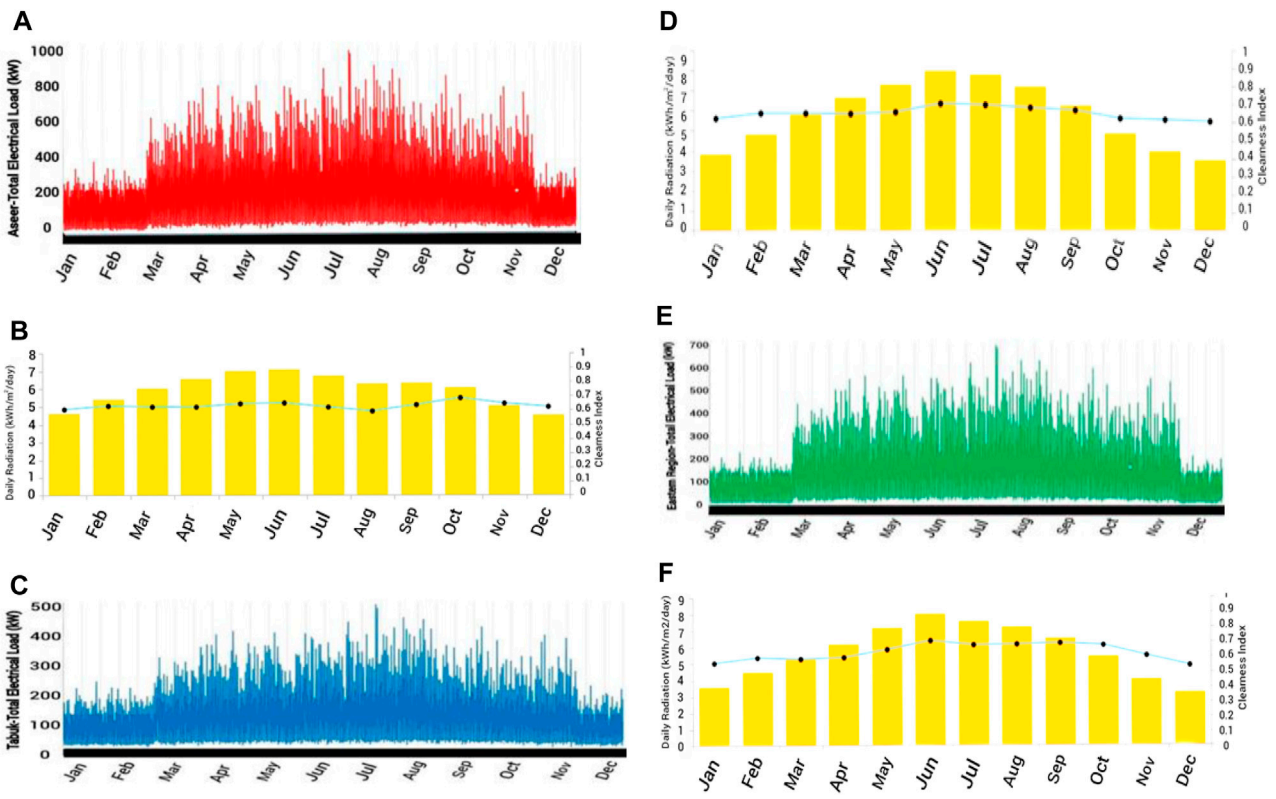

FIGURE 5 | (A) Annual load profile for selected case study located in Aseer. **(B)** Solar radiation and clearness index in Aseer. **(C)** Annual load profile for selected case study located in Tabuk province. **(D)** Solar radiation and clearness index in Tabuk province. **(E)** Annual load profile for selected case study located in Eastern Region province. **(F)** Solar radiation and clearness index in Eastern Region province.

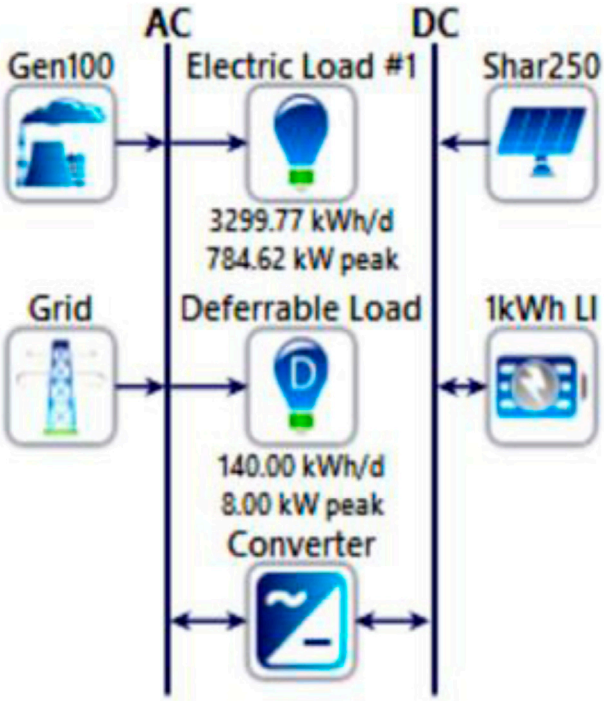

FIGURE 6 | Schematic view of the proposed system.

Accordingly, each household's share in electricity usage was 43.3 kWh/day, that is, 18.2 kWh/day in winter and 25 kWh/day for the rest of the year in 2017 (Survey, 2017). The latitude and longitude of the selected case study region in this province are 28°N, 36°E, respectively.

In **Figure 5C**, like Aseer, the deferrable load is assumed to be 140 kWh/day and demand load is 2,346 kWh/day, that is, 1,820 kWh/day in winter and 2,500 kWh/day for the rest of the days. The mentioned values are applied to HOMER software's defined distribution load demand for residential usages. Based on the obtained values, peak times occur in June–October at 1–6 p.m. Solar radiation and clearness index for this province are shown in **Figure 5D**, where average radiation is considered to be 5.84 kWh/m^2/day.

2.5.5 Eastern Region

The biggest province in Saudi Arabia is the Eastern Region, where households were 758,916 in number, and total electricity consumption was 11 billion kWh/year. According to the conducted survey (Survey, 2017), electricity consumption on average for each household was 56 kWh/day, that is, 19 kWh/day in winter and 37 kWh/day for the rest of the year in 2017. It includes almost all of the entire southeast and east of the country. Since this province is so long, its middle part with the latitude of 26°N and longitude of 49°E is selected as the case study region as marked in **Figure 4**.

The distribution of demand load is shown in **Figure 5E**, and it is similar to the Aseer and Tabuk provinces except for winter months; during the rest of the year, electricity consumption is significant. For this case study, the deferrable load is assumed to be 140 kWh/day and on average 3,299 kWh/day, so that 19 kWh/day in Winter and 39 kWh/day for the rest of the year are considered and imposed on the default load in HOMER software for residential usage. Also, the solar radiation of 5.72 kWh/m^2/day is averagely set for this case study. Solar radiation and clearness index in this province are presented in **Figure 5F**.

2.6 The Proposed Hybrid System, Assumptions, and Components

For all of the case studies, the proposed system is shown in **Figure 6**. It includes PV, DG, battery, converter, grid, electrical, and deferrable load. It must be mentioned that the value of considered demand load for each city is set in HOMER according to an almost equal number of households for all three selected case studies based on the consumption reported through the conducted survey in 2017.

The characteristics of the components and input parameters are presented in **Table 2**, where the project's lifetime is considered to be 20 years. Since the loads are based on residential usage, annual capacity shortage, as a percent of blackout which can occur in a year, should be considered about 1%–2%. However, in this study, simulations are done for three annual capacity shortages, including 0%, 1%, and 2%, to see the differences between results and select the rational annual capacity shortage for the rest of the study. The discount and inflation rates are considered to be 6% and 3%, respectively. Also, PV panels include the Horizontal Tracker system.

2.6.1. Components' Technical Description

2.6.1.1 Photovoltaic Panels

In HOMER software, **Eq. 3** is used to calculate the output power from PV panels where it considers both environmental and structural factors such as wind speed and solar radiation.

The output power of PV is as follows:

$$PV = RC^{*}DF^{*}\left(\frac{SRI}{IR}\right)*[1 + TCP*(CT - CT_{STC})] \quad (3)$$

where RC presents rated capacity(kW) of PV considering the Standard Test Condition (STC). DF is defined as the derating factor (%) of PV. SRI is the Solar Radiation Incident (kW/m^2) in the current time step. TCP is the temperature coefficient of power (%/°C). CT and CT_{STC} are PV's cell temperature (°C) at reality and STC, respectively.

2.6.1.2 Converter

Usually, most PV panels produce DC current that cannot be used directly in residential applications. This equipment is used to convert DC current to AC. The details of the selected converter are described in **Table. 2**.

2.6.1.3 Battery

Increasing the reliability of the power generation systems is an essential factor, especially in peak hours when pressure on the grid is significant. Using batteries can release this pressure by supplying demand load when it is necessary, especially in blackouts and night hours when there is no solar irradiation.

TABLE 2 | Characteristics of the proposed components.

Component	PV	DG	Converter	Battery
Model	Sharp ND-250QCS	Generic Medium Genset	—	1 kWh Li-Ion
Capital cost ($/kW)	1,500	450	300	400
Replacement ($/kW)	1,200	380	300	400
O&M ($/year)	30	18	6	10
Lifetime	20 years	15,000 h	15 years	15 years
Cell type	Polycrystalline silicon	—	—	—
Operating temperature	47.5°C	—		
Temperature coefficient	−0.485%/°C	—	—	—
Efficiency	15.3%	—	95%	90%
Minimum load ratio	—	25%	—	—
Rated RPM	—	1,500	—	—
Nominal capacity	0.25 kW	0, 5, 10, 15 kW	—	1 kWh-167 Ah
Nominal voltage	—	—	—	6 V
Charge and discharge current	—	—	—	167, 500 A

The characteristics of the selected battery in this study are presented in **Table. 2**.

2.6.2. Economic Equations in HOMER

2.6.2.1 Net Present Cost (NPC)

HOMER software's total net present cost is calculated as in **Eq. 4**. It includes all the expenses that are spent on the project, such as initial capital, operation and maintenance, fuel, replacement cost, and other related expenses. It also considers the project's income (salvage) throughout its lifetime.

$$NPC = \frac{C_{initial} + C_{replecement} + C_{O\&M} - Salvage}{CRF(i,n)} \quad (4)$$

where CRF is the capital recovery factor that can be calculated through **Eq. 5**, and n is the project's lifetime (years). **Eq. 6** presents *i*, where f is the specific inflation rate and *i* and *i*' are real and nominal interest rates, respectively.

$$CRF(i,n) = \frac{i(1+i)^n}{(1+i)^n - 1} \quad (5)$$

$$i = \frac{i' - f}{1+f} \quad (6)$$

2.6.2.2 Cost of Energy (COE)

The cost of energy of the project is defined as **Eq. 7**. It means how much money is spent for generation of 1 kWh electricity and is calculated by dividing the system's total annualized cost by the total electrical load (kWh/year).

$$COE = \frac{CRF(i,n) * C_{NPC}}{E_{served,\ ACprime} + E_{served,DCprime} + E_{seved,def} + E_{grid,sales}} \quad (7)$$

where $E_{served,me}$ $E_{served,ACprime}$ are the total energy spent on DC and AC loads, $E_{grid,sales}$ is the amount of energy sold to the grid, and $E_{seved,def}$ is the served deferrable load of the system.

2.6.3 Grid Electricity Prices and Employed Constraints

Considering load profiles in **Figures 5A,C,E** and electricity consumption for all case studies based on the reported survey in 2017, power usage is significantly lower than that in the rest of the year in the winter months. Accordingly, consumption is considered shoulder mode for December, January, and February. For the rest of the year, three different modes are assumed so that 11 p.m. to 7 a.m. is considered off-Peak hours and the rest of the day is considered as shown in **Figure 7A**. The prices of grid sales and purchases for three modes are presented in **Figure 7B**. The other assumption in this study is the constant blackouts in the peak hours of the day, especially in June, July, August, and September, coupled with ten random blackouts where each one is 30 min. In order to reduce pressure on the grid, constant grid blackouts are just assumed since supplying electricity in peak hours of the day using renewable energies is one of this study's goals. For July, August, and September, 2 and 3 p.m. are considered, and for the rest of the non-winter months, 1 h between 2 and 3 p.m. is deemed to be shown in **Figure 7C**.

2.6.4 Grid Pollutant Emission

About 97% of the total electricity generation in eastern parts of Saudi Arabia is through natural gas; however, due to the lack of gas pipelines in the western regions, almost all power generation is based on petroleum liquids (U.S. EIA, 2021). Some studies considered grid pollutant emission as follows: 632 g/kWh of carbon dioxide, 1.79 g/kWh of carbon monoxide, 0.2 g/kWh of unburned hydrocarbons, 0.14 g/kWh of particular matter, 1.47 g/kWh of sulfur dioxide, and 1.60 g/kWh of nitrogen oxides (Tazay, 2020). It should be mentioned that about 28% of total CO_2 emission in Saudi Arabia is related to the power sector. Also, 65% of total fuel for electricity generation is natural gas and the rest (35%) is from oil (U.S. EIA, 2021; Climate Transparency Report, 2020). In this study based on the kind of fuels used in each region of Saudi Arabia and other related reports of power plants' emission, CO_2 emission of the grid is considered to be 850 g/kWh and 550 g/kWh for the western and eastern regions of Saudi Arabia, respectively. Also, based on a conducted study in the United States, the social cost of CO_2, CH_4, and N_2O emission are considered to be 40, 1,500, and 17,000 $/t (U. S. Government, 2013).

3 RESULTS AND DISCUSSION

In this section, machine learning results and optimization results are presented in two separate parts.

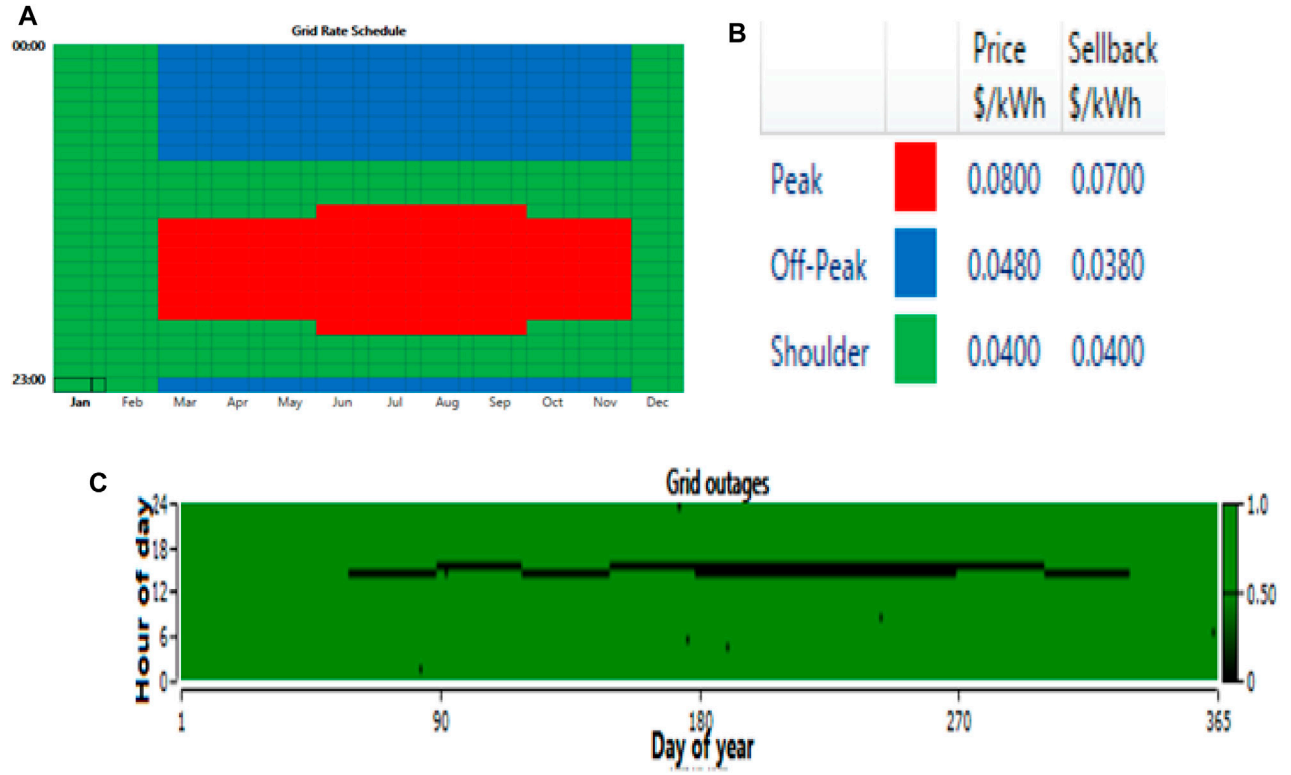

FIGURE 7 | (A) Grid rate schedule. **(B)** Purchase (from) and sale (to) grid prices. **(C)** Assumed random and constant grid outages.

TABLE 3 | Results of MLP and SVR methods.

Method	R2	MAE	Input parameters	Goal
MLP	0.996	2.3	Learning rate: 0.1/alpha:0.005/solver: lbfgs Layers:2/nodes:20	CO_2 prediction
SVR	0.991	2.8	Kernel: poly/degree:3/epsilon:0.1	
MLP	0.98	4.1	Learning rate: constant/alpha:0.02/solver: lbfgs/layers:1/nodes:9	Electricity prediction
SVR	0.99	3.3	Kernel: poly/degree:3/epsilon:0.1	

3.1 Estimated CO_2 Emission and Electricity Consumption

There are some criteria through which the accuracy of regression methods is evaluated. In this study, R^2 and MAE are employed. Considering similar studies in which prediction is made by using MLP and SVR methods, the obtained R^2s and MAEs are acceptable (Ghalandari et al., 2020; Fan et al., 2021). In **Table 3**, results of MLP and SVR methods for predicting CO_2 emission and electricity consumption are presented. Different kernels such as linear, RBF, and polynomials were used in the SVR method, and it was concluded that polynomials had better performance for the current data. As it can be seen for CO_2 emission, MLP has higher R2 and lower error than SVR, while for prediction of electricity consumption, SVR has shown better accuracy. Accordingly, MLP and SVR are employed to predict CO_2 emission and electricity consumption, respectively.

The outputs of the models are shown in **Figures 8A,B**. Considering the predicted outputs of predicted CO_2 emission and electricity consumption, the rate of increasing emission is 9.5 Mt/year and that for electricity consumption is 6.3 TWh/year. It means that if the dependent parameters such as GDP, population, and oil consumption grow according to **Figures 3A–H**, CO_2 emission and electricity consumption will increase by 31% and 39%, respectively, by 2040 compared to 2020. Hence, using renewable energies should be higher than CO_2 emission and electricity consumption rates.

3.2 Simulation Results

In this section, the obtained outputs of HOMER software are presented and discussed. First, results, including the optimized components' sizes, emission, and economic parameters, are shown in **Table 4** under three different annual capacity shortages. Second, three sensitivity analyses, including the amount of CO_2 emission coupled with its penalties, amount of

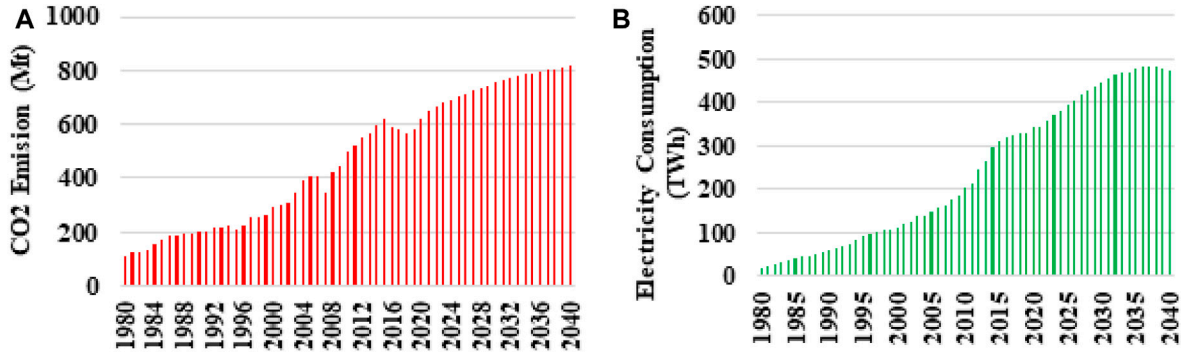

FIGURE 8 | (A) Predicted CO_2 emission by MLP. **(B)** Predicted electricity consumption by SVR.

TABLE 4 | Obtained results under three different annual capacity shortages—Aseer, Tabuk, and the Eastern Region.

Aseer										
Annual capacity shortage (%)	**COE ($/kWh)**	**NPC ($)**	**Initial capital ($)**	**RF (%)**	**PV (kW)**	**Battery (kW)**	**Gen (kW)**	**CO_2 emission (kg/yr.)**	**Unmet load (kWh/yr.)**	**Capacity shortage (kWh/yr.)**
0	0.0934	2.57M	1.03M	48	507	411	5	809,510	305	1,559
1	0.0949	2.52M	895,899	44.6	447	323	5	834,642	822	5,102
2	0.0949	2.52M	901,030	44.8	454	317	5	832,268	801	4,807
Tabuk										
0	0.0915	1.37M	511,984	46.2	257	178	5	457,998	9.05	422
1	0.0907	1.37M	514,992	46.7	257	173	5	457,161	12.2	512
2	0.0907	1.37M	514,992	46.7	257	173	5	457,161	12.2	512
Eastern										
0	0.0910	1.91M	760,062	46.7	380	271	5	411,209	3.04	1,225
1	0.0922	1.90M	716,545	44.8	358	265	5	417,963	67	2,200
2	0.0922	1.90M	719,545	44.8	358	265	5	417,963	67	2,200

solar GHI and load, and the price of PV and battery, are done for the best-selected capacity shortage according to the previous section to see RF and NPC changes. Finally, technical analyses of the optimized systems are presented.

3.2.1 Optimized Systems for Aseer, Tabuk, and Eastern Region

The outputs of the proposed system under three annual capacity shortage values are presented in **Table 4**. Considering the literature review in the introduction section, where the RFs are between 32% and 50%, the corresponding COEs are between 0.049 ($/kWh) and 0.178 ($/kWh). Comparing the obtained COEs with similar on-grid studies in Saudi Arabia shows that the COEs are rational (Alharthi et al., 2018; Al Garni et al., 2018; Awan et al., 2019; Dehwah and Krarti, 2019).

- In Aseer, COE values show 0.0015 $/kWh increase for 1% and 2% capacity shortage compared to 0% while NPC is 0.05M($) lower for 1% and 2% shortage compared to 0%. RF in 0% shortage is 48% while 44.6% and 44.8% values are obtained for 1% and 2% shortage, respectively, which show 6% decrease compared to 0% shortage. Consequently, PV capacity is obtained as 11% and 10% lower in 1% and 2% shortages compared to the other one. CO_2 emission is also 3% and 2.8% lower in 0% shortage compared to 1% and 2% shortages, respectively. Also, unmet load in 1% and 2% is 1.7 and 1.6 times higher in 1% and 2% shortages compared to 0% shortage.
- In Tabuk, comparison of COEs shows a 0.0008 $/kWh increase in 1% and % shortages compared to 0% shortage while NPC has not been changed at all. Also, RF, the size of PV, batteries, Gen, and other parameters have not had any significant change and are almost equal for all three considered shortages.
- In the Eastern Region, a 0.0002 $/kWh decrease happens for COE of 0% shortage compared to two other shortages while NPC for 0% shortage is 0.01M($) more than the other shortages. Comparison of RF values shows 4% increase in 1% and 2% shortages compared to 0% shortage. Consequently, the size of PV for 0% shortage is 271(kW),

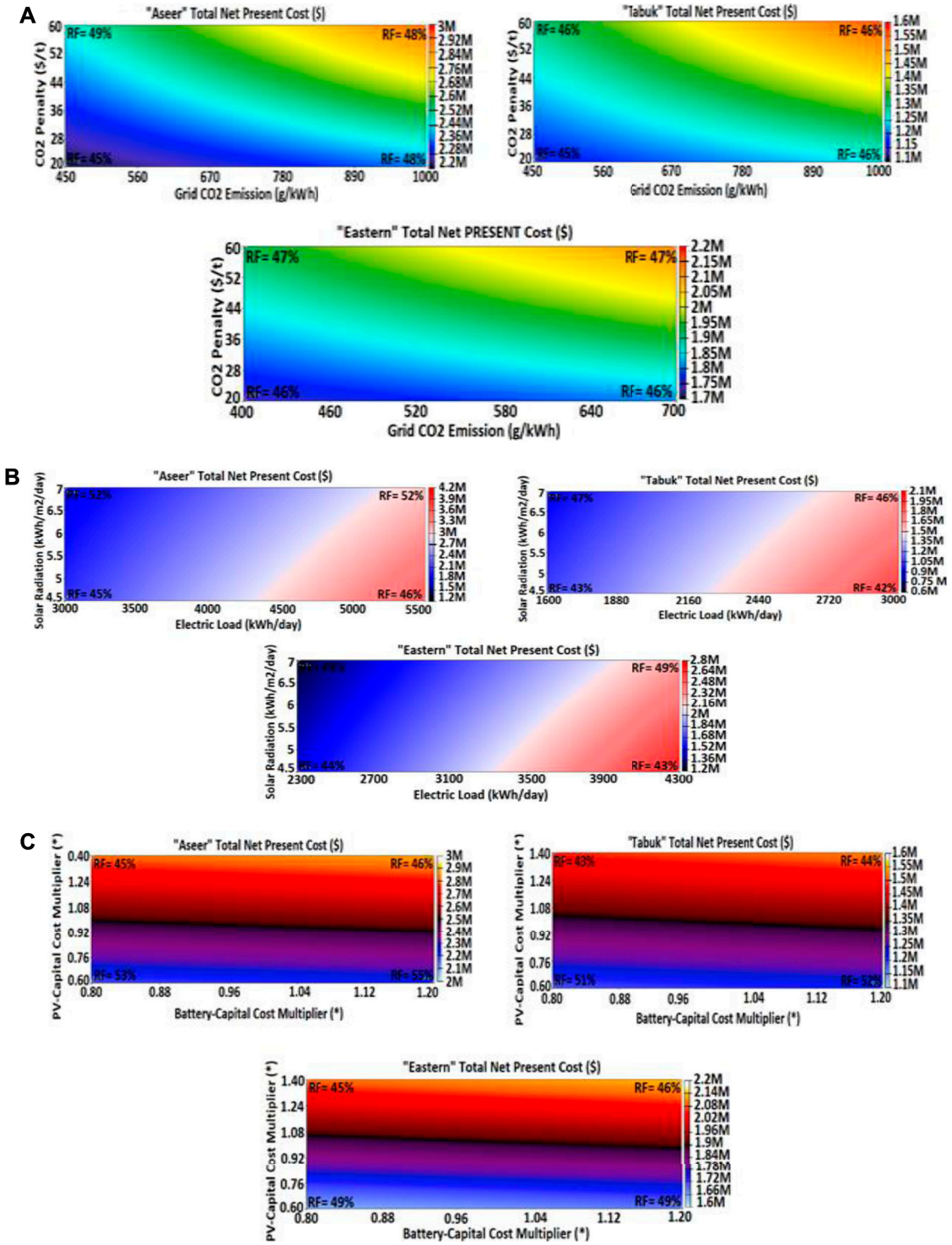

FIGURE 9 | (A) Sensitivity analysis on the grid CO_2 emission and its social penalties. **(B)** Sensitivity analysis on solar GHI and Load. **(C)** Sensitivity analysis on the price of PV and battery.

which is 2% higher than 1% and 2% shortages. Results show a 1% increase in CO_2 emission for 1% and 2% shortages compared to 0% shortage. Also, unmet load for 1% and 2% shortage is 22 times more than 0% shortage.

The optimized results, based on the economic parameters, especially NPC and COE values, show that increasing annual capacity shortage have not had a significant effect on the NPC and COE and will not change the size of components, while its impact

on the unmet electricity are remarkable and CO_2 emission will be higher. Hence, it would be rational to select a 0% annual capacity shortage for supplying power with the lowest unmet electricity. Considering equal obtained RFs (46–48) % and equal households for all cases, the PV panels' size for supplying electricity in Aseer, Tabuk, and the Eastern Region is 507, 257, and 380 kW, respectively. The size of DG for all cases is obtained as 5 kW, and it will be used just as a small essential backup.

3.2.2 Sensitivity Analysis on the Amount of Grid CO_2 Emission and Its Penalty-0% Shortage

In this section, 450–1,000 g/kWh CO_2 emission is considered for Aseer and Tabuk provinces as the cases using petroleum liquids for power production and 400–700 g/kWh CO_2 is considered for the Eastern Region since it is using natural gas as fuel. For all cases, penalties' ranges are considered to be 20–60 $/t according to the mentioned study in the grid pollutant emission section. Heat maps in **Figure 9A** show the obtained results.

- According to this figure for Aseer, reducing CO_2 emission by 450 g/kWh (e.g., using natural gas in this area) while CO_2 penalty is 20 $/t, 45% RF would be enough with an NPC of 2.2M($). However, if the penalty is 60 $/t, 49% RF will be the optimized value and increase NPC by 14%. Also, the results show that by increasing CO_2 by 1,000 g/kWh along with 60 $/t of CO_2 penalty, the RF of 48% will not be changed in optimization while NPC will be 36% higher than when 20 $/t is the penalty. Changes in CO_2 emission from 450–1,000 g/kWh, where the penalty is 20 $/t, will not significantly affect NPC, while RF will be increased 45%–48%.
- Changes in CO_2 and its penalty for Tabuk province would lead to 45% RF where CO_2 emission is decreased by 450 g/kWh and 20 $ penalty while considering 60$/t penalty, 46% RF is enough, and it increases NPC by 18%. Here, the emission is 1,000 g/kWh and changing the penalty from 20 to 60 $/t will not affect RF, while NPC will be increased by about 24%. Considering 20 $/t penalty and changing emission from 450 to 1,000 g/kWh would lead to 45% and 46% RF and increase in NPC by 13%. Also, where the penalty is 60 $/t, changing emission from 450 to 1,000 g/kWh caused 46% RF and increased NPC by 24%.
- The Eastern Region shows different treatment compared to Aseer and Tabuk. For CO_2 emission of 400 g/kWh, changing the penalty from 20 to 60 $/t caused 46% and 47% RF and increased NPC by 15%. Also, when the emission is 1,000 g/kWh, changing the penalty from 20 to 60 $/t caused 46% and 47% RF and increased NPC by 20%. Where CO_2 emission of the grid is changed from 400 to 700 g/kWh and penalty is 20 $/t, the constant value of 46% and 1.7M ($) for RF and NPC are the best values, respectively. Where the social penalty is 60 $/t, 47% of RF will be selected as the optimum value for the range of 400–700 g/kWh emission, but it increases NPC by 30%.

3.2.3 Sensitivity Analysis on Solar GHI and Electrical Load-0% Shortage

In order to see the effect of various loads and solar GHIs on RF and NPC, sensitivity analysis was conducted, and results are presented in **Figure 9B**. The ranges for loads are 30% different from primary annual averages, including 4,266, 2,346, and 3,300 kWh/day for Aseer, Tabuk, and the Eastern Region, respectively. Also, solar GHI is set to 4.5 to 7 kWh/m^2/day near most parts of Saudi Arabia.

- In Aseer province, where the load is 3,000 kWh/day, 4.5—7 kWh/m^2/day GHI caused 45% and 52% RF, respectively, while NPC has not been changed. For the 5,500 kWh/day load, changing GHI from 4.5 to 7 kWh/m^2/day caused 46% and 52% RF, respectively, and decreased NPC by about 5%. Changing the load between 3,000 and 5,500 kWh/day where GHI is 4.5 kWh/m^2/day increases RF from 45% to 46% and the value of NPC by about 55%. Where GHI is 7 kWh/m^2/day, changing the load between 3,000 and 5,500 kWh/day will not affect RF, but it will increase the NPC by 43%.
- In Tabuk province, where demand load is 1,600 kWh/day, having 4.5 and 7 kWh/m^2/day values of GHI causes 43% and 47% RF, respectively, and NPC will not change more than 5%. In loads near 3,000 kWh/day, changing GHI from 4.5 to 7 kWh/m^2/day would result in 42% and 46% RF, respectively, and decrease NPC by 4%. If the location has had 4.5 kWh/m^2/day radiation and the load changes from 1,600 to 3,000 kWh/day, RF will be almost constant (42.5%) while NPC will be increased by about 50%. For GHIs of about 7 kWh/m^2/day, optimum obtained RFs for loads between 1,600 and 3,000 kWh/day are about 46.5%, while the NPC increases up to 66%.
- The sensitivity analysis results for the Eastern Region show that where the load is 2,300 kWh/day, changing GHI from 4.5 to 7 kWh/m^2/day causes 44% and 49% RF while NPC has almost a constant value of 1.3M ($). Also, where the load is 4,300 kWh/day, the range of 4.5–7 kWh/m^2/day for GHI would cause 43% and 49% RF, respectively, and decreases NPC by about 12%. Where GHI has a constant value of 4.5 kWh/m^2/day, the range of 2,300–4,300 kWh/day demand load has an almost constant value of RF (43.5%) while NPC will be increased by 70%. Also, in GHIs, about 7 kWh/m^2/day RF will be constant (49%), while NPC increases about 60%.

3.2.4 Sensitivity Analysis on the Price of PV and Battery- 0% Shortage

One of the most important issues for designing hybrid renewable systems is the price of components. Following the obtained results in **Table 4**, PV and battery are the main parts of the optimized systems.

Hence, in this section, for all selected case studies for the capital cost of PV and battery, 40% and 20% tolerance are considered, respectively, to see the changes in RFs and NPCs as shown in **Figure 9C**.

- In Aseer province, by reducing 20% of the capital cost of batteries for the range of 0.6–1.4 of PV's capital cost, RF changes from 53% to 45%, and NPC increases by 65%. Also, when the capital cost of batteries is 1.2 times more, altering the price of PV by 0.6–1.4 of the capital cost would result in 55% and 46% RFs, respectively, and increase NPC by about 70%. The changes in the batteries' price will not significantly affect RFs and NPCs.

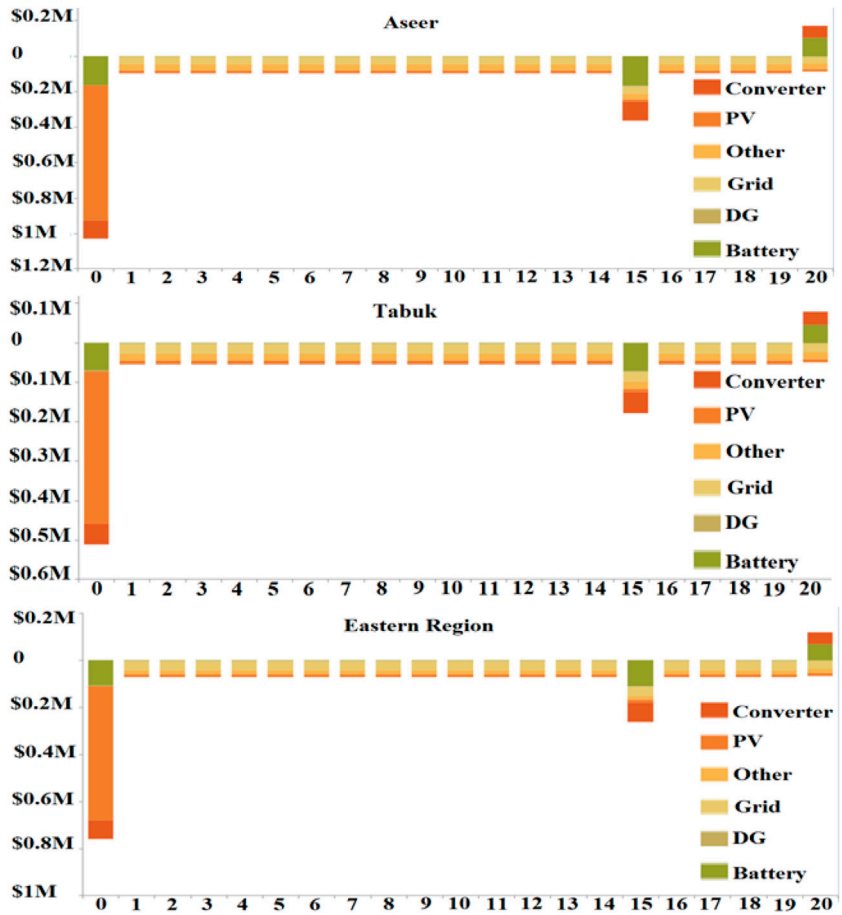

FIGURE 10 | Cash flow diagrams, including components' cost in 20 years.

- In Tabuk province, if the price of batteries decreases by 20%, for the range of 0.6–1.4 of the prices of PV, the optimum RFs will be 51% and 43%, respectively, and NPC will increase by 25%. Also, if the price of batteries increases by 20%, increasing the capital cost of PVs by 0.6–1.4 would result in 52% and 44% RFs and increase the NPC by 30%. Like Aseer province, changing battery prices by 20% does not significantly affect RFs and NPCs.
- Obtained results for the Eastern Region show that a 20% reduction of the price of batteries and changing the price of PVs in the ranges of 0.6–1.4 times of the capital cost would cause 49% and 45% RFs and increase the NPC by about 28%. Also, if the price of batteries increases by 20% and the price of PVs changes from 0.6 to 1.4 times the capital cost, RFs will be 49% and 46%, respectively, and the NPC will be increased by about 33%. Changing the price of batteries by 20% will not affect RFs and NPCs as well.

3.3 Technical Analysis and Cash Flow Diagrams

For all the case studies, cash flow diagrams along the project's lifetime (20 years) are illustrated in **Figure 10**. Initial capital cost includes most of the total NPC, and the maximum capital cost is related to PV in all cases. Also, at year 15, batteries and converters need to be replaced. The other important issue inferred from this figure is that at the end of the project, such components as batteries and converters will remain that can be sold to the market, which is considered salvage. As mentioned before, the generator has less cost among the components and will not be replaced over the 20 years.

The load and power generation of the selected case studies along with grid purchases and sales are shown in **Figure 11** for a typical week. Considering the fixed and random blackouts of the grid at peak times, PV panels will supply outages between 2 and 3 p.m., and if the random outages occur at night, batteries can provide the demand loads. As shown in **Figure 11**, DG is not being used, so it is only used as a backup component so that when the batteries could not provide all of the demand load, DG would help them supply electricity. Take the curve of Aseer's technical analysis on August 18, 3 p.m., as an example; at this time, one of the blackouts has occurred, and grid purchase is at its minimum state while PV is generating electricity and batteries are helping it.

At this specific time, since the PV is exposed to intense radiation in addition to the supplying demand load, it can sell the excess electricity to the grid. Taking Tabuk's performance

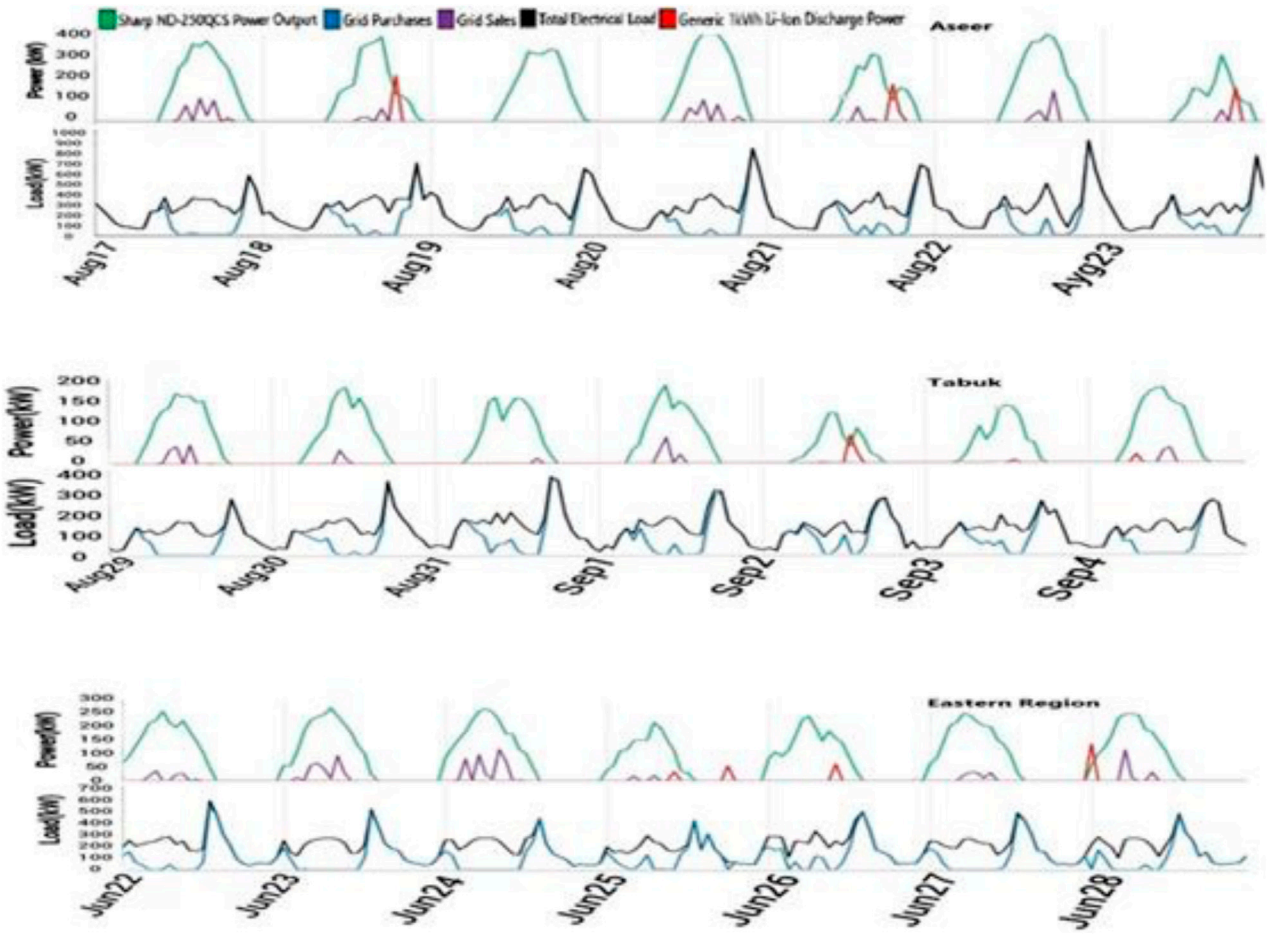

FIGURE 11 | Technical performance of the optimized systems in a typical week.

curves into account on September 2 at 4 p.m., it is shown that when outages finish, batteries have a significant role in providing electricity at the begging time of the grid exposed to intense radiation; in addition to the supplying demand load, it can sell the excess electricity to the grid. Taking Tabuk's performance curves into account on September 2 at 4 p.m., it is shown that when outages finish, batteries have a significant role in providing electricity at the begging time of grid connection while PV's power is not enough. The last state of the battery's usage is when one of the random grid outages (30 min) occurs.

As seen in the Eastern Region's curves on June 25 at 9 p.m., batteries are lonely supplying the demand load when there is no other component helping them. In this study, charging batteries through the grid and selling from the battery to the grid are prohibited. For this reason, all of the sales to the grid occur when PVs are generating electricity.

4 CONCLUSION AND FUTURE WORK

In this work, the results of machine learning methods employed to predict CO_2 emission and electricity consumption in Saudi Arabia by 2040 showed that the rates of increasing CO_2 emission and electricity consumption were 6.3 Mt/year and 9.5 TWh/year, respectively. In the prediction process, such essential factors as GDP, oil consumption, and population are considered. This study investigates grid-connected hybrid renewable systems under different annual capacity shortages when there are fixed grid outages and random ones. Aseer, Tabuk, and the Eastern Region of Saudi Arabia are selected as three coastal provinces so that demand loads are 4,266, 2,346, and 3,300 kWh/day, respectively. In order to find the best range of RFs for each province, some sensitivity analyses are employed under changes of grid CO_2 emission and its penalties, demand load and solar GHI, and PV and batteries' capital cost. Considering all the assumptions and input parameters in this study, the most important findings are as follows:

- MLP and SVR methods showed more accuracy for predicting CO_2 emission and electricity consumption, respectively. Also, results showed that the increasing rate of using renewable energies should support 31% increasing CO_2 emission and 39% electricity consumption by 2040 compared to 2020.

- Despite having residential usage, considering 0% annual capacity shortage has no significant impact on the financial results and the size of components compared to 1% and 2% yearly capacity shortage. Also, unmet electricity is highly affected when 1% and 2% shortages are considered and increases up to 1.5–22 times more than 0% shortages in addition to increasing CO_2 emission in Aseer and the Eastern Region.
- The range of 46%–48% RF would be the best for all cases from economic and environmental points of view.
- A PV/Battery system including a partial amount of DG as a backup supplier would be the best combination for all cases. Also, COEs of the optimized system for Aseer, Tabuk, and the Eastern Region are 0.0934, 0.0915, and 0.0910 $/kWh, respectively. Furthermore, RFs of the mentioned cases are 48%, 46.2%, and 46.7%, respectively.
- Overall, changes in grid CO_2 emission and its social penalty (20–60$) do not change the optimum value of RFs, while increasing one or both will significantly increase the NPC values for all case studies.
- Considering the different loads and GHIs (4.5–7 kWh/m^2/day), the ranges of 45%–52%, 42%–47%, and 43%–49% RFs in Aseer, Tabuk, and the Eastern Region, respectively, while the range of loads for these cases is 3,000–5,500 kWh/day, 1,600–3,000 kWh/day, and 2,300–4,300 kWh/day, would lead to an optimum system.
- Sensitivity analysis on the price of PV and battery when the range of the battery's cost is 320–480 $/kW, and PV's price range is 900–2,100 $/kW shows that the optimum ranges of RFs for Aseer, Tabuk, and the Eastern Region are 45%–55%, 43%–52%, and 45%–49%, respectively. Also, it was found that changing the battery price at the mentioned ranges will not affect NPC, while PV's prices will significantly change the NPC values.

For future work, we suggest using other renewable energies such as wind and bio-power. Investigating various kinds of trackers can also be considered.

DATA AVAILABILITY STATEMENT

The original contributions presented in the study are included in the article/Supplementary Material, further inquiries can be directed to the corresponding author.

AUTHOR CONTRIBUTIONS

All authors listed have made a substantial, direct, and intellectual contribution to the work and approved it for publication.

FUNDING

Funded by the Deanship of Scientific Research of University of Hafr Al Batin (UHB), Hafr Al Batin, Saudi Arabia, through research grant no: 0054-S1443.

ACKNOWLEDGMENTS

The authors would like to acknowledge the support of the Deanship of Scientific Research of University of Hafr Al Batin (UHB), Hafr Al Batin, Saudi Arabia, through research.

REFERENCES

Al Garni, H. Z., Awasthi, A., and Ramli, M. A. M. (2018). Optimal Design and Analysis of Grid-Connected Photovoltaic under Different Tracking Systems Using HOMER. *Energ. Convers. Management.* 155, 42–57. doi:10.1016/j.enconman.2017.10.090

Alharthi, Y., Siddiki, M., and Chaudhry, G. (2018). Resource Assessment and Techno-Economic Analysis of a Grid-Connected Solar PV-Wind Hybrid System for Different Locations in Saudi Arabia. *Sustainability.* 10, 3690–3710. doi:10.3390/su10103690

Almasri, R. A., and Narayan, S. (2021). A Recent Review of Energy Efficiency and Renewable Energy in the Gulf Cooperation Council (GCC) Region. *Int. J. Green Energ.* 18 (14), 1441–1468. doi:10.1080/15435075.2021.1904941

Altikat, S. (2021). Prediction of CO2 Emission from Greenhouse to Atmosphere with Artificial Neural Networks and Deep Learning Neural Networks. *Int. J. Environ. Sci. Technol.* 18 (10), 3169–3178. doi:10.1007/s13762-020-03079-z

Awan, A. B. (2019). Performance Analysis and Optimization of a Hybrid Renewable Energy System for Sustainable NEOM City in Saudi Arabia. *J. Renew. Sustain. Energ.* 11 (2), 25905. doi:10.1063/1.5071449

Awan, A. B., Zubair, M., Sidhu, G. A. S., Bhatti, A. R., and Abo-Khalil, A. G. (2019). Performance Analysis of Various Hybrid Renewable Energy Systems Using Battery, Hydrogen, and Pumped Hydro-Based Storage Units. *Int. J. Energ. Res.* 43 (12), 6296–6321. doi:10.1002/er.4343

Bamisile, O., Obiora, S., Huang, Q., Yimen, N., Abdelkhalikh, I., Cai, D., et al. (2021). Impact of Economic Development on CO2 Emission in Africa; the Role of BEVs and Hydrogen Production in Renewable Energy Integration. *Int. J. Hydrogen Energ.* 46 (2), 2755–2773. doi:10.1016/j.ijhydene.2020.10.134

Barhoumi, E. M., Okonkwo, P. C., Zghaibeh, M., Belgacem, I. B., Alkanhal, T. A., Abo-Khalil, A. G., et al. (2020). Renewable Energy Resources and Workforce Case Study Saudi Arabia: Review and Recommendations. *J. Therm. Anal. Calorim.* 141 (1), 221–230. doi:10.1007/s10973-019-09189-2

Buyukyildiz, M., Kahramanli, H., and Tezel, G. (2013). "Application of Support Vector Regression (SVR) for Monthly Evaporation Prediction," in proceedings of the 4th European Conference of Civil Engineering (ECCIE '13) Proceedings of the 1st European Conference of Mining Engineering (MINENG '13), Antalya, Turkey, October 8–10, 2013.

Climate Transparency Report (2020). Saudi Arabia, Country Profile. Available at: https://www.climate-transparency.org/media/saudi-arabia-country-profile-2020.

Dehwah, A. H. A., and Krarti, M. (2019). Optimal Hybrid Power Energy Systems for Residential Communities in Saudi Arabia. *J. Sol. Energ. Eng.* 141 (6), 61002. doi:10.1115/1.4043633

El Haj Assad, M., Mahariq, I., Al Barakeh, Z., Khasawneh, M., and Ali Amooie, M. (2021). Modeling CO2 Emission of Middle Eastern Countries Using Intelligent Methods. *C. Mater. Contin.* 69 (3), 3767–3781. doi:10.32604/cmc.2021.018872

Eltamaly, A. M., Ali, E., Bumazza, M., Mulyono, S., and Yasin, M. (2021). Optimal Design of Hybrid Renewable Energy System for a Reverse Osmosis Desalination System in Arar, Saudi Arabia. *Arab. J. Sci. Eng.* 46 (10), 9879–9897. doi:10.1007/s13369-021-05645-0

Fan, G.-F., Yu, M., Dong, S.-Q., Yeh, Y.-H., and Hong, W.-C. (2021). Forecasting Short-Term Electricity Load Using Hybrid Support Vector Regression with Grey Catastrophe and Random forest Modeling. *Utilities Policy*. 73, 101294. doi:10.1016/j.jup.2021.101294

Forootan Fard, H., Khodaverdi, M., Pourfayaz, F., and Ahmadi, M. H. (2020). Application of N-Doped Carbon Nanotube-Supported Pt-Ru as Electrocatalyst Layer in Passive Direct Methanol Fuel Cell. *Int. J. Hydrogen Energ.* 45 (46), 25307–25316. doi:10.1016/j.ijhydene.2020.06.254

Ghalandari, M., Forootan Fard, H., Komeili Birjandi, A., and Mahariq, I. (2020). Energy-related Carbon Dioxide Emission Forecasting of Four European Countries by Employing Data-Driven Methods. *J. Therm. Anal. Calorim.* 144, 1999–2008. doi:10.1007/s10973-020-10400-y

Heydari, A., Garcia, D. A., Keynia, F., Bisegna, F., and Santoli, L. D. (2019). Renewable Energies Generation and Carbon Dioxide Emission Forecasting in Microgrids and National Grids Using GRNN-GWO Methodology. *Energ. Proced.* 159, 154–159. doi:10.1016/j.egypro.2018.12.044

Ibrahim, M. S., Dong, W., and Yang, Q. (2020). Machine Learning Driven Smart Electric Power Systems: Current Trends and New Perspectives. *Appl. Energ.* 272, 115237. doi:10.1016/j.apenergy.2020.115237

IEA (2021). *Global Energy Review 2021*. Paris: IEA. Available at: https://www.iea.org/reports/global-energy-review-2021.

Kharrich, M., Kamel, S., Alghamdi, A. S., Eid, A., Mosaad, M. I., Akherraz, M., et al. (2021). Optimal Design of an Isolated Hybrid Microgrid for Enhanced Deployment of Renewable Energy Sources in Saudi Arabia. *Sustainability.* 13 (9), 4708. doi:10.3390/su13094708

Ming, H., Xia, B., Lee, K.-Y., Adepoju, A., Shakkottai, S., and Xie, L. (2020). Prediction and Assessment of Demand Response Potential with Coupon Incentives in Highly Renewable Power Systems. *Prot. Control. Mod. Power Syst.* 5 (1), 1–14. doi:10.1186/s41601-020-00155-x

Nishan, M. K. A. (2020). Role of Energy Use in the Prediction of CO2 Emissions and Economic Growth in India: Evidence from Artificial Neural Networks (ANN). *Environ. Sci. Pollut. Res.* 27 (19), 23631–23642.

Qu, S., Cai, H., Xu, D., and Mohamed, N. (2021). Uncertainty in the Prediction and Management of CO2 Emissions: a Robust Minimum Entropy Approach. *Nat. Hazards* 107 (3), 2419–2438. doi:10.1007/s11069-020-04434-6

Ramezanizadeh, M., Alhuyi Nazari, M., Ahmadi, M. H., Lorenzini, G., and Pop, I. (2019). A Review on the Applications of Intelligence Methods in Predicting thermal Conductivity of Nanofluids. *J. Therm. Anal. Calorim.* 138 (1), 827–843. doi:10.1007/s10973-019-08154-3

Salameh, T., Sayed, E. T., Abdelkareem, M. A., Olabi, A. G., and Rezk, H. (2021). Optimal Selection and Management of Hybrid Renewable Energy System: Neom City as a Case Study. *Energ. Convers. Management* 244, 114434. doi:10.1016/j.enconman.2021.114434

Sayed, E. T., Wilberforce, T., Elsaid, K., Rabaia, M. K. H., Abdelkareem, M. A., Chae, K.-J., et al. (2021). A Critical Review on Environmental Impacts of Renewable Energy Systems and Mitigation Strategies: Wind, Hydro, Biomass and Geothermal. *Sci. Total Environ.* 766, 144505. doi:10.1016/j.scitotenv.2020.144505

Seedahmed, M. M. A., Ramli, M. A. M., Bouchekara, H. R. E. H., Shahriar, M. S., Milyani, A. H., and Rawa, M. (2022). A Techno-Economic Analysis of a Hybrid Energy System for the Electrification of a Remote Cluster in Western Saudi Arabia. *Alexandria Eng. J.* 61 (7), 5183–5202. doi:10.1016/j.aej.2021.10.041

Shabani, E., Hayati, B., Pishbahar, E., Ghorbani, M. A., and Ghahremanzadeh, M. (2021). A Novel Approach to Predict CO2 Emission in the Agriculture Sector of Iran Based on Inclusive Multiple Model. *J. Clean. Prod.* 279, 123708. doi:10.1016/j.jclepro.2020.123708

Singh, A., Kotiyal, V., Sharma, S., Nagar, J., and Lee, C.-C. (2020). A Machine Learning Approach to Predict the Average Localization Error with Applications to Wireless Sensor Networks. *IEEE Access* 8, 208253–208263. doi:10.1109/access.2020.3038645

Singh, P. K., Pandey, A. K., Ahuja, S., and Kiran, R. (2021). Multiple Forecasting Approach: a Prediction of CO2 Emission from the Paddy Crop in India. *Environ. Sci. Pollut. Res.* 1, 1–12. doi:10.21203/rs.3.rs-767860/v1

Survey, H. E. (2017). "Household Energy Survey 2017," in *General Authority for Statistics*, 1–288.

Taylan, O., Alamoudi, R., Kabli, M., AlJifri, A., Ramzi, F., and Herrera-Viedma, E. (2020). Assessment of Energy Systems Using Extended Fuzzy AHP, Fuzzy VIKOR, and TOPSIS Approaches to Manage Non-cooperative Opinions. *Sustainability.* 12 (7), 2745. doi:10.3390/su12072745

Tazay, A. F., Samy, M. M., and Barakat, S. (2020). A Techno-Economic Feasibility Analysis of an Autonomous Hybrid Renewable Energy Sources for University Building at Saudi Arabia. *J. Electr. Eng. Technol.* 15 (6), 2519–2527. doi:10.1007/s42835-020-00539-x

Tazay, A. (2020). Techno-Economic Feasibility Analysis of a Hybrid Renewable Energy Supply Options for University Buildings in Saudi Arabia. *Open Eng.* 11 (1), 39–55. doi:10.1515/eng-2021-0005

Tee, P. F., Abdullah, M. O., Tan, I. A. W., Rashid, N. K. A., Amin, M. A. M., Nolasco-Hipolito, C., et al. (2016). Review on Hybrid Energy Systems for Wastewater Treatment and Bio-Energy Production. *Renew. Sustainable Energ. Rev.* 54, 235–246. doi:10.1016/j.rser.2015.10.011

U.S. Eia (2021). Country Analysis Executive Summary: Saudi Arabia. *U.S. Energ. Inf. Adm. Indep. Stat. Anal.*, 9. [Online]. Available at: https://www.eia.gov/international/content/analysis/countries_long/Saudi_Arabia/saudi_arabia.pdf.

U. S. Government (2013). Technical Support Document: Technical Update of the Social Cost of Carbon for Regulatory Impact Analysis under Executive Order 12866. *Soc. Cost Carbon Estim. Regul. Impact Anal. Dev. Tech. Assess.*, 65–88. [Online]. Available at: https://www.epa.gov/sites/default/files/2016-12/documents/sc_co2_tsd_august_2016.pdf.

Wu, B., Maleki, A., Pourfayaz, F., and Rosen, M. A. (2018). Optimal Design of Stand-Alone Reverse Osmosis Desalination Driven by a Photovoltaic and Diesel Generator Hybrid System. *Solar Energy* 163, 91–103. doi:10.1016/j.solener.2018.01.016

Xu, H., Pan, X., Guo, S., and Lu, Y. (2021). Forecasting Chinese CO2 Emission Using a Non-linear Multi-Agent Intertemporal Optimization Model and Scenario Analysis. *Energy* 228, 120514. doi:10.1016/j.energy.2021.120514

Zhang, Y., Han, J., Pan, G., Xu, Y., and Wang, F. (2021). A Multi-Stage Predicting Methodology Based on Data Decomposition and Error Correction for Ultra-short-term Wind Energy Prediction. *J. Clean. Prod.* 292, 125981. doi:10.1016/j.jclepro.2021.125981

Zhu, C., Wang, M., and Du, W. (2020). Prediction on Peak Values of Carbon Dioxide Emissions from the Chinese Transportation Industry Based on the SVR Model and Scenario Analysis. *J. Adv. Transp.* 2020, 2020. doi:10.1155/2020/8848149

Conflict of Interest: The authors declare that the research was conducted in the absence of any commercial or financial relationships that could be construed as a potential conflict of interest.

Publisher's Note: All claims expressed in this article are solely those of the authors and do not necessarily represent those of their affiliated organizations, or those of the publisher, the editors, and the reviewers. Any product that may be evaluated in this article, or claim that may be made by its manufacturer, is not guaranteed or endorsed by the publisher.